12 (2022) 100261

Contents lists available at ScienceDirect

Biosensors and Bioelectronics: X

journal homepage: www.journals.elsevier.com/biosensors-and-bioelectronics-x

Electrochemical impedance biosensor for Chagas Disease diagnosis in clinical samples

J.S. Cisneros [a], C.Y. Chain [a,*], M.A. Daza Millone [a], C.A. Labriola [b], K. Scollo [c], A.M. Ruiz [c], P. Estrela [d], M.E. Vela [a]

[a] Instituto de Investigaciones Fisicoquímicas Teóricas y Aplicadas (INIFTA-UNLP-CONICET), La Plata, Argentina
[b] Fundación Instituto Leloir, Instituto de Investigaciones Bioquímicas de Buenos Aires (IIBBA-CONICET), Universidad Nacional de Buenos Aires, Argentina
[c] Instituto Nacional de Parasitología "Dr. Mario Fatala Chabén" - Administración Nacional de Institutos y Laboratorios de Salud (ANLIS), Buenos Aires, Argentina
[d] Centre for Biosensors, Bioelectronics and Biodevices (C3Bio) and Department of Electronic & Electrical Engineering, University of Bath, Calverton Down, Bath BA2 7AY, United Kingdom

ARTICLE INFO

Keywords:
Immunosensor
Impedimetric sensor
Chagas disease
Cruzipain
Self-assembled monolayers
Clinical samples

ABSTRACT

Chagas disease (CD) is one of the main neglected tropical diseases, diagnosed mainly by serological tests performed in centralized laboratories, which severely limits the clinical management of the disease in communities with scarce resources. Herein, an electrochemical impedance biosensor for the detection of CD was developed for the first time using a cruzipain-based sensor surface. The protein, highly immunogenic and isolated from *Trypanosoma cruzi*, was immobilized over the surface of gold disc electrodes modified with 11-mercaptoundecanoic (MUA) and 6-mercapto-1-hexanol (MCH) self-assembled monolayers (SAMs). Reproducible sensor surfaces, yielding 38 ± 3% coverage as measured by Surface Plasmon Resonance, were obtained by amide coupling of 120 μg/mL cruzipain onto 1/10 MUA/MCH SAMs for 30 min. Under optimized operational conditions, the impedimetric immunosensor recognized specific interactions for anti-*T. cruzi* antibodies in 1/800 diluted human serum patient samples. The charge transfer resistance of the biosensors increases by ~18% in the presence of the positive samples, whereas the negative samples give rise to a negligible increase of around 6%. An excellent selectivity to clinical samples from patients infected with *T. cruzi* was obtained. The clear signal difference obtained for positive and negative clinical samples highlights the applicability of the sensors for the point-of-care diagnosis of CD.

1. Introduction

Chagas disease (CD) is currently one of the main neglected tropical diseases, affecting 7 million people all over the world. At the beginning of the 20th century, CD was an endemic condition in South America, Central America and Mexico and the main mode of transmission was through bloodsucking insects infected with *Trypanosoma cruzi* (*T. cruzi*) (Rassi et al., 2010). Nowadays, CD is widespread in non-endemic regions including European countries, Canada and USA (Lidani et al., 2019) and the vertical transmission of the disease is responsible for many new CD cases.

The diagnosis of CD is mainly based on the detection of specific anti *T. cruzi* antibodies that appear early in serum after the parasitic infection of a patient (Balouz et al., 2017). The commonly used serological methods to detect CD are indirect hemagglutination (IHA), indirect immunofluorescence (IFF) and enzyme-linked immunosorbent assay (ELISA), most of them relying on crude or semi purified extracts of the parasite or recombinant proteins as ligands. A serum sample is considered positive for CD when two or three of the mentioned serological methods are positive as, until now, the indirect diagnosis of CD does not have a reliable gold standard, i.e. a unique serological test offering a definite result. Purified proteins isolated from *T. cruzi* are not frequently used as ligands (Balouz et al., 2017), although they have all the native antigenic sites, as opposed to recombinant proteins that only mimic natural macromolecules.

During the past few decades, several impedimetric biosensors with promising applications in medical point of care detection (POCT) have been reported (Leva-Bueno et al., 2020; Singh et al., 2018; Sypabekova et al., 2019), including Electrochemical Impedance Spectroscopy (EIS) immunoassays for the diagnosis of CD, based on semi purified antigenic

* Corresponding author.
E-mail address: yamil@inifta.unlp.edu.ar (C.Y. Chain).

https://doi.org/10.1016/j.biosx.2022.100261
Received 23 August 2022; Received in revised form 26 September 2022; Accepted 28 September 2022
Available online 6 October 2022

fractions (Santos et al., 2016) or recombinant antigens of *T. cruzi* (Cordeiro et al., 2020; Diniz et al., 2003). Among the strategies that have been developed for the fabrication of impedimetric immunosensors (Leva-Bueno et al., 2020), the use of self-assembled monolayers (SAMs) onto gold surfaces continues to be an advantageous choice for ligand immobilization. Mixed thiol SAMs, containing a thiol with carboxylic terminal groups together with a short thiol, i) allow to achieve reproducible covalent immobilizations of amine-containing bioreceptors (Hermanson, 1997), ii) increase the bio-stability of the ligands in comparison with non-functionalized gold, iii) create an adequate dielectric layer between the surface and the media (Campuzano et al., 2006) and iv) permit to control the density of ligands onto the sensor surface (Chen et al., 2014).

We have recently developed an optical biosensor for the diagnosis of CD by immobilizing an isolated protein from *T. cruzi*, cruzipain (CrP), onto a gold surface. CrP (Cazzulo et al., 1997) is highly immunogenic (Cazorla et al., 2010) and the presence of anti-CrP antibodies have been verified in serum samples from patients with chronic CD (Martinez et al., 1991). The obtained Surface Plasmon Resonance (SPR) immunosensor was tested with clinical samples infected with *T. cruzi*, showing a good correlation with the results obtained by ELISA based in crude parasite extracts (Chain et al., 2019). Encouraged by these findings and to move towards miniaturization of the detection method, in this work we developed an impedimetric sensor surface based on CrP for the diagnosis of CD. Different platforms were obtained and qualitatively and quantitatively characterized by cyclic voltammetry (CV) and SPR. A reproducible sensor platform based on CrP was obtained and was successfully used to discriminate between clinical serum samples infected and not infected with *T. cruzi*. The present study brings innovations to this scientific area since the impedimetric detection of CD by means of a *T. cruzi* isolated protein enables the construction of low-cost portable CD biosensors.

2. Material and methods

2.1. Reagents

CrP was obtained from crude *T. cruzi* epimastigote Y strain extracts by affinity chromatography (Labriola et al., 1993). N-hydroxysuccinimide (NHS), ethanolamine hydrochloride, N-(3-(dimethylamino)-propyl)-N′-ethylcarbodiimide hydrochloride (EDC), phosphate buffered saline (0.01 M PBS, pH 7.4) tablets, potassium hexacyanoferrate (III), potassium hexacyanoferrate (II) trihydrate, 11-mercapto-undecanoic acid (MUA) and 6-mercapto-1-hexanol (MCH) were of analytical grade and purchased from Sigma-Aldrich, UK. Absolute ethanol (HPLC grade) and Startingblock™ Blocking buffer were purchased from Fisher Scientific (UK) and potassium hydroxide was purchased from J.T.Baker (UK). Electrode polishing kit was obtained from BASi Inc. (Japan). All aqueous solutions were prepared using 18.2 MΩ cm ultra-pure water with a Pyrogard filter (Millipore, UK).

2.2. Apparatus and electrochemical measurements

EIS and CV were recorded using a μAutolab III/FRA2 or an Autolab PGSTAT12/FRA2 potentiostat connected to a computer with NOVA 2.1 software (Metrohm, The Netherlands) and a PalmSens PS4 potentiostat with PSTrace software (PalmSens, Netherlands). A three-electrode cell with Ag/AgCl (3 M KCl) reference electrode (BASi, USA) connected via a salt bridge filled with buffer and platinum counter electrode (ALS, Japan) was used for all measurements. The electrochemical impedance spectrum was measured in a PBS buffer containing 2 mM ferro/ferricyanide $[Fe(CN)_6]^{3-/4-}$ redox couple. The frequency range used for the measurement was 10 kHz–100 mHz, with a 10 mV AC voltage superimposed on a bias DC voltage of 0.2 V vs Ag/AgCl, corresponding to the formal potential of the redox couple. All measurements were performed at room temperature.

2.3. Electrode surface preparation

Gold disc working electrodes with 3 mm diameter (BASi, IN, USA) were cleaned mechanically as described in Sypabekova et al. (2019). Briefly, the mechanical cleaning started by a sonication in absolute ethanol (10 min), followed by a 2 min manual polishing first over 1 μm diamond powder and then with 0.05 μm alumina slurry polishing pads. After each step the electrodes were sonicated in absolute ethanol (2 min) and milli-Q water (10 min). In order to remove compounds that were not completely eliminated by polishing, electrodes were electrochemically cleaned in 50 mM KOH by scanning the potential between −0.2 V and +1.2 V versus Ag/AgCl for 15–20 cycles (scan rate of 50 mV/s). Cyclic voltammetry in this potential range removes surface imperfections or contaminations due to the oxidation/reduction of gold atoms together with the oxidation of remaining organic compounds, including thiols. Finally, the electrodes were thoroughly rinsed with Milli-Q water and dried under a stream of N_2 and stored in PBS until use (no more than a few hours).

The first step in the construction of the sensing platform was the formation of mixed SAMs on the gold disc electrodes (Scheme 1). The working electrodes were incubated overnight at RT with a 250 μL mixture of 50 μM MUA and 50 μM MCH (1/100 or 1/10 vol ratio) in ethanol. The electrodes were then gently rinsed with ethanol and water and incubated successively in 0.1 M EDC/NHS (30 min) in milliQ-water and in CrP solution in PBS (30 or 60 min). After rinsing the electrodes with the measurement buffer to remove any unattached CrP, a blocking step was performed with either 1 M ethanolamine or Startingblock™ blocking buffer (30 min) in order to block any unreacted carboxylic group and to diminish non- specific interactions. The prepared sensors were then placed into the measurement buffer with 2 mM ferro/ferricyanide $[Fe(CN)_6]^{3-/4-}$ redox couple for at least 1 h for surface stabilization.

2.4. Human sera

Archived human serum samples were obtained from individuals either chronically infected or not infected with *T. cruzi* from Instituto Nacional de Parasitologia (INP) “Dr. Mario Fatala Chabén” (Buenos Aires, Argentina). Serological diagnosis of clinical samples was performed with ELISA, IHA and IFF with “in-house” antigens (whole cells for IFA and crude cell extracts for IHA and ELISA), compliant with domestic and international rules.

The preliminary evaluation of the CrP sensor platform for EIS-based immunosensing was carried out with 12 human sera samples divided into two pools: one consisting of 6 sera from individuals infected with *T. cruzi* (positive pool) and another of 6 sera from individuals not infected (negative pool). Serum samples were 1/100 and 1/800 diluted in PBS before EIS measurements.

2.5. SPR measurements

Measurements were performed using a SPR Navi™ 210A (BioNavis, Finland) instrument operating with two independent flow channels. The temperature of the experiments was kept constant at 22 °C, the flow rate was 10 μL/min and PBS was employed as running buffer. Mixed MUA/MCH SAMs were obtained by overnight incubation of the SPR gold substrates (BioNavis, Finland), equivalent to gold electrode modification described in Section 2.3. SPR substrates were cleaned by immersion in H_2O_2:NH_3:H_2O 1:1:2 mixture at ~90 °C during 5 min and washed with Milli-Q and absolute ethanol prior to use.

SPR sensorgrams for CrP immobilization were assayed for both 1/100 and 1/10 MUA/MCH Au SAMs. MUA/MCH-Au surfaces were functionalized with a mixture of 0.010 M EDC and 0.015 M NHS (10 min), 107 μg/mL CrP (15 min) and 1 M ethanolamine, pH 8.5 (10 min). This *in situ* immobilization was monitored by the variation of SPR peak minimum angle (Θ_{SPR}). The SPR minimum angle variation ($\Delta\Theta_{SPR}$)

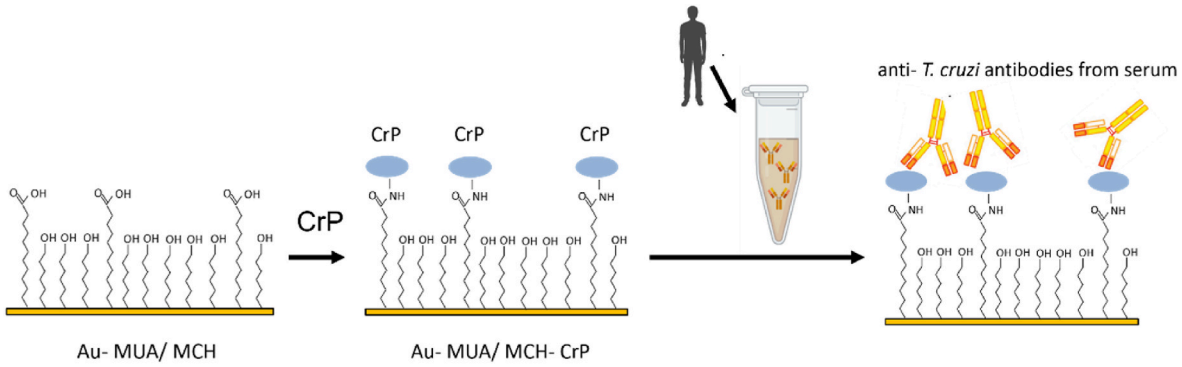

Scheme 1. Schematic illustration of the different steps involved in the obtention of the sensor platform.

assigned to the immobilization of CrP corresponds to the difference between the value of Θ_{SPR} detected at $t = 0$ and after blocking and washing procedures. Measurements were made in duplicate and surface coverages were estimated according to de Feijter equation as described by Chain et al. (2019).

3. Results and discussion

3.1. Construction of the sensor platform

The nature of the antigens used as ligands in anti-*T. cruzi* assays have an important relevance on the specificity of the detection (World Health 2010). Scheme 1 presents a schematic overview of the sensor surface modifications applied in this study, which include CrP isolated from *T. cruzi* as ligand that is covalently immobilized onto carboxylic thiol SAMs.

We have previously reported the development of a sensor surface for the optical biosensing of anti-*T. cruzi* antibodies as biomarkers of CD (Chain et al., 2019). The platform was built from a gold substrate covered with a single thiol SAM (of 3-mercaptopropionic acid), where CrP was covalently bound via amide coupling. CrP immobilization parameters were followed in real time and optimized, reaching a surface coverage of 35%. The SPR biosensor based in CrP could discriminate between positive and negative CD cases, showing an excellent agreement with ELISA in serum samples diluted 1/800 in PBS.

Some operational parameters used to construct the CrP-based SPR sensor platform (Chain et al., 2019) were optimized for the obtention of the impedimetric sensor platform described in the current study. The CrP-based EIS sensor surface was prepared by successive incubations with MUA/MCH, EDC/NHS, CrP and ethanolamine solutions. The involved volumes in each step were higher in the present biosensor (0.75 mL in comparison with 0.4 mL in the SPR surface), with the aim to cover the gold disc electrode surface. The incubation times with 1) EDC/NHS, 2) CrP, 3) ethanolamine and 4) serum samples were longer (30 min in each step) in the EIS biosensor compared with the SPR biosensor (10 min, 20 min, 10 min and 10 min, respectively) to take into account possible differences between the static incubation (present work) and the incubation under flow conditions in the former SPR development (Chain et at. 2019).

3.2. Characterization of the sensor platform

To evaluate the electron transfer properties of the bare gold disc electrode in comparison with the obtained sensor surface, CV measurements were carried out. Fig. 1A shows the cyclic voltammograms for the gold disc electrode in the presence of the redox probe before and after the functionalization with CrP (orange and blue curves, respectively). A reversible redox couple typical of a diffusion-limited process is observed in the bare electrode (orange curve). The CrP-functionalized electrode (blue curve) exhibits, on the other side, a more irreversible electron transfer and a decrease in the anodic and cathodic current peaks, compatible with the immobilization of the protein onto the sensor surface.

Characteristic Nyquist plots for the Au disc electrode before functionalization (orange curve), after the self-assembly of the thiol SAM (black curve) and after the immobilization of CrP (blue curve) are presented in Fig. 1B. Important variations in R_{ct} (read as a diameter of the semicircle from the Nyquist plots) are observed depending on the chemical modifications that the Au-disc electrode suffers during the preparation of the CrP based sensor surface.

The experimental data was fit using a Randles equivalent circuit model that is shown as inset in Fig. 1B), in which R_s is the solution resistance, CPE the constant phase element, R_{ct} the charge transfer resistance and W the Warburg impedance to model diffusion. The gold disc electrode shows a small value for resistance of charge transfer ($R_{ct} = 0.900 \pm 0.004$ kΩ) (orange curve in Fig. 1B), typical of metallic surfaces. The increase in R_{ct} (2.090 ± 0.001 kΩ) (black curve in Fig. 1B) observed in EDC/NHS-MUA/MCH-Au SAMs reveals the partial hindering of charge transfer due to the deposition of the thiol SAM and subsequent chemical activation of the carboxylic groups. CrP

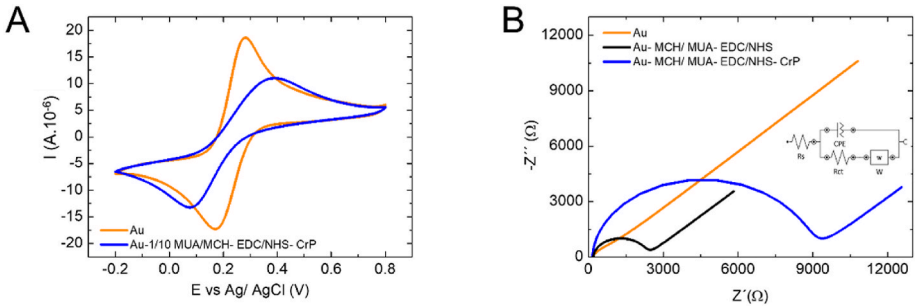

Fig. 1. A) Representative cyclic voltammograms obtained for bare electrode and for the obtained sensor platform (last of 5 cycles shown) in $[Fe(CN)_6]^{3-/4-}$ (2 mM in PBS, 50 mV/s). B) Impedimetric characterization of the build-up process of the CrP-based sensor platform.

immobilization leads to a further increase in R_{ct} (8.662 ± 0.001 kΩ) (blue curve in Fig. 1B), verifying that the platform was sensitive to antigen immobilization, as it will be verified by SPR (seesection 3.3.1).

3.3. Optimization of the platform design

3.3.1. MUA/MCH volume ratio

Different MUA/MCH concentration ratios have been reported for the fabrication of biosensors (Chen et al., 2014; Hushegyi et al., 2015). The concentration and distribution of the carboxylic groups in the organic layer onto the Au surface govern, among others, the efficacy of the posterior ligand immobilization.

In this work, Au surfaces were functionalized by incubation with 1/100 or 1/10 vol ratios of 50 μM MUA and MCH ethanolic solutions (to give account of distinct carboxylic density and distribution), followed by an activation with EDC/NHS and an incubation with CrP solutions of different concentrations (24 μg/mL and 120 μg/mL, respectively) to take into consideration the different amounts of carboxylic groups in each case. A long incubation time (60 min) with CrP solution was chosen in order to ensure that CrP immobilization was not kinetically limited.

Black columns in Fig. 2 show the R_{ct} values for MUA/MCH-Au SAMs before CrP immobilization. The lower R_{ct} (2.4 ± 0.4 kΩ) obtained in 1/10 MUA/MCH-Au SAMs can be explained in terms of the higher amount of MUA ionizable carboxylic groups that increases the conductivity of the interface when compared with 1/100 MUA/MCH-Au SAMs (R_{ct} = 5.1 ± 0.8 kΩ). After CrP immobilization, R_{ct} showed, within experimental error, the same mean values for both mixed MUA/MCH-Au SAMs (blue columns in Fig. 2), in accordance with SPR results (discussed in the paragraph). Concerning the reproducibility of CrP immobilization, the surface chemistry based on 1/100 diluted SAM showed a higher dispersion in R_{ct} of CrP (32.8% RSD) in comparison with immobilization based in 1/10 MUA/MCH (8.7% RSD). This finding can be related with the higher number of SAM configurations that can arise if the long thiol (MUA) is highly diluted in MCH and in the variability of the thiol-surface coverage of the independent experiments, which spreads in a highly variable immobilization sites available for CrP. From these experiments, it is clear that 1/10 MUA/MCH and 120 μg/mL CrP is the choice for the subsequent measurements, although it is possible that CrP concentration could be further decreased in order to reduce the cost per assay.

To monitor the evolution of the bound mass onto gold surfaces as functionalization steps occur, SPR studies were performed. Red and black curves in Fig. 3 correspond to the sensorgrams characterizing covalent immobilization of CrP onto 1/10 and 1/100 MUA/MCH-Au

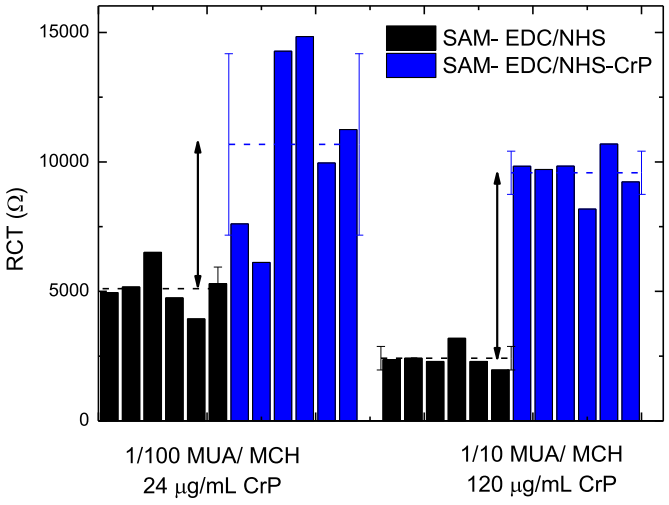

Fig. 2. R_{ct} for 1/100 and 1/10 activated MUA/MCH Au SAMs before and after 60 min CrP immobilization (error bars represent the SD obtained for six electrodes).

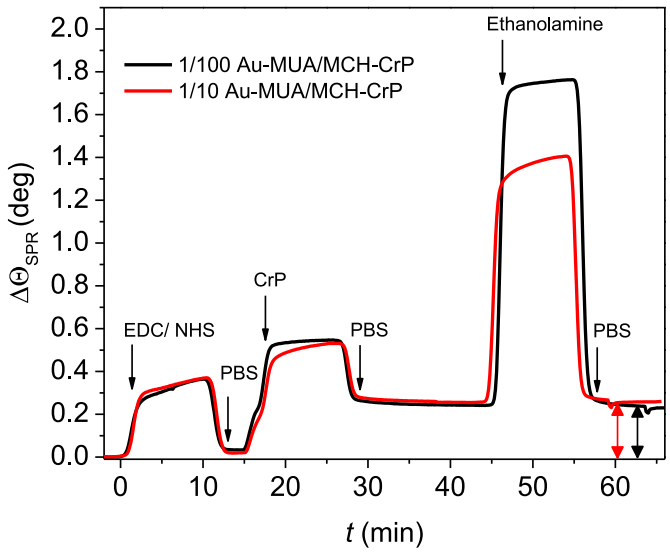

Fig. 3. SPR sensorgrams showing CrP immobilization on 1/10 and 1/100 MUA/MCH-Au SAMs (arrows indicate $\Delta\Theta_{SPR}$ for CrP immobilization in each case).

SAMs, respectively. As it can be seen, the successive steps in ligand immobilization leads to an increase in the SPR signal, verifying that CrP can be effectively bounded to the Au surface in these experimental conditions. The obtained $\Delta\Theta_{SPR}$ (that is, the difference between Θ_{SPR} detected at $t = 0$ and after the blocking step) can be related to the surface coverage through de Feijter equation (Chain et al., 2019). The surface coverage calculation yields 35 ± 1% (onto 1/100 MUA/MCH) and 38 ± 3% (onto 1/10 MUA/MCH) of the surface covered by CrP (considering a close packed array as 100% of coverage); a fact that is compatible with an adequate ligand−analyte interaction. These results verified that the degree of CrP immobilization is virtually the same in the two mixed SAMs. Moreover, the same surface coverage was obtained in the SPR sensor platform based in CrP developed by this group (Chain et al., 2019), obtained by immobilization of 120 μg/mL CrP during 20 min.

3.3.2. CrP incubation time

Once defined the optimal MUA/MCH vol ratio, the possibility to shorten CrP incubation time was studied. With this goal, six different electrodes (prepared from 1/10 MUA/MCH ethanolic solutions and activated with 0.1 M EDC/NHS) were incubated during 30 and 60 min with 120 μg/mL CrP in PBS and subsequently blocked with Starting-block™ blocking buffer or ethanolamine solution, as previously described.

Shorter incubation times with CrP yields sensor surfaces with the same impedances (mean $R_{ct} = 9 \pm 2$ kΩ) than those arising from 60 min incubations (mean R_{ct} = 9.5 ± 0.9 kΩ), verifying a saturation of the surface after 30 min incubation with CrP solution. Based on these results and in order to achieve fast detections, 30 min incubation time is recommended for the construction of the CrP-based EIS immunosensor platform.

3.4. Selectivity of CrP-based sensor platform towards T. cruzi infected serum samples

After the tuning of CrP immobilization onto the Au disc electrodes, the performance of the CrP-based sensor platform for the impedimetric detection of anti-*T. cruzi* antibodies in clinical samples was assessed. With this aim, functionalized electrodes were incubated during 30 min at room temperature with a pool of both negative and positive sera diluted 1/100 or 1/800 in PBS. After gently washing the surface with PBS buffer, impedance measurements were carried out.

EIS measurements on 1/800 serum dilutions in PBS (but not 1/100 dilutions) allowed to discriminate between positive and negative samples, possibly due to the reduction of non-specific binding in more diluted serum. This result is in accordance with the optimum dilution factor of the CrP-based SPR immunosensor (Chain et al., 2019). Fig. 4A shows typical Nyquist plots of CrP-modified electrode before (blue curve) and after the immersion in positive (green curve) and negative serum (red curve). R_{ct} shows a negligible increase after the incubation with negative samples when compared to the CrP-functionalized electrode, in contrast to the noticeable R_{ct} increase after the incubation with the positive serum.

Fig. 4B shows the results obtained for the R_{ct} variation ($\Delta R_{ct} = R_{ct,serum} - R_{ct,CrP}$) of CrP-modified gold disc electrodes after the incubation with serum samples. The observed 18% increase in R_{ct} values after the incubation with the positive samples is significantly larger than the 5.8% increase observed with the negative sample.

Furthermore, impedance measurements using the developed sensor were able to distinguish between clinical samples positive and negative for *T. cruzi* infection at 1/800 serum dilution factor, in comparison with 1/400 dilution factor that is frequently used in ELISA (Chain et al., 2019), indicating that an EIS immunosensor based in CrP-functionalized gold disc electrodes can be a sensitive method to diagnose CD.

Finally, to determine the repeatability of the immunosensor, relative standard deviation (RSD) values were calculated. Positive samples were detected with four different electrodes in three independent experiments under the optimized conditions, with RSD values of 24, 35, 17 and 8%. This indicates that a moderate reproducibility of the immunodetection of anti- *T. cruzi* antibodies is achievable in the present operational parameters.

3.5. Comparison of the developed assay with other detection methods based in CrP

Since its first description in the early 1990s (Murta et al., 1990), CrP has been widely used as ligand in ELISA at the laboratory-scale with the aim to elucidate details of the molecular paths involved in the pathogenesis and immune response to *T. cruzi* infection (Giordanengo et al., 2002). ELISAs involved the physical adsorption of the ligand onto special wells, a blocking step (usually performed with serum albumin) and two extra chemical reactions to label the antigen-antibody complex. In this sense, the incubation with a second antibody conjugated to an enzyme and the subsequent reaction with a substrate of the enzyme, implies several chemical reagents and the need of a centralized laboratory to read the result of the chemical reaction by means of a spectrophotometer. Although highly specific detections of CD were reported with CrP-based ELISA (Malchiodi et al., 1994), the use of CrP as ligand in immunoassays for the detection of CD is not widespread (Flores-Chavez Maria et al., 2018), possibly due to the existence of well-established recombinant ligands (World Health 2010) and in the fact that CrP is nowadays highly studied as potential chemotherapeutic agent for the disease (Cerny et al., 2020).

To move towards the portable detection of CD and taking into consideration the advantages of CrP as ligand, we reported a CrP-based SPR biosensor (Chain et al., 2019), based in the covalent immobilization of the protein, that showed an excellent correlation with the results obtained with an ELISA based in semi purified extracts of *T. cruzi*. The present CrP-based EIS biosensor was successfully developed on the basis of the previous report. The mean $\Delta R_{ct\ POS} = 1.8 \pm 0.3$ kΩ and mean $\Delta R_{ct\ NEG} = 0.6 \pm 0.2$ kΩ obtained in the CrP-based EIS immunosensor are in accordance with the results obtained with the CrP-based SPR immunosensor (Chain et al., 2019) in which the increase in SPR signal after incubation with positive serum (mean $\Delta\Theta_{SPR} = 0.075°$) was three times higher than SPR response after the addition of negative serum (mean $\Delta\Theta_{SPR} = 0.025°$). The present development means an advance in the field of CD diagnosis, as the CrP-based EIS biosensor can be miniaturized (Ibau et al., 2020) in order to get POCT.

4. Conclusions

We developed an impedimetric immunoassay for the detection of anti- *T. cruzi* antibodies in diluted serum patient samples. The sensor platform presents advantageous characteristics: i) it uses a highly immunogenic protein from *T. cruzi* as ligand, ii) it is based on thiol SAMs, a well-known method that yields reproducible ligand immobilizations and iii) it implies short preparation times. Concerning the immunodetection of anti- *T. cruzi* antibodies, as the levels of anti- *T. cruzi* on the patient samples obtained are unknown, we currently cannot determine the limits of detection of the system. However, an excellent selectivity to clinical samples from patients suffering from CD is verified. Positive clinical samples show a positive signal of around 18% increase in R_{ct}, while control samples show a negligible signal.

The results obtained with the biosensor are extremely promising and tests with more clinical samples, including those infected with other pathogens usually sources of false positives results, might produce further information in terms of specificity of the detection. Moreover, due to the features of this development, miniaturization of the biosensors is easily achievable, which combined with recent progress on low-cost portable potentiostats, might in the future bring the impedimetric detection of anti-CrP antibodies towards the POCT of CD.

CRediT authorship contribution statement

J.S. Cisneros: Methodology, Formal analysis, Investigation, Writing – review & editing. **C.Y. Chain:** Conceptualization, Methodology, Formal analysis, Investigation, Writing – original draft, Writing – review & editing, Project administration, Funding acquisition. **M.A. Daza Millone:** Methodology, Formal analysis, Investigation, Writing – review & editing. **C.A. Labriola:** Conceptualization, Resources. **K. Scollo:** Conceptualization, Resources. **A.M. Ruiz:** Conceptualization, Resources. **P. Estrela:** Conceptualization, Methodology, Resources, Writing – review & editing, Supervision, Funding acquisition. **M.E. Vela:** Conceptualization, Methodology, Resources, Writing – review &

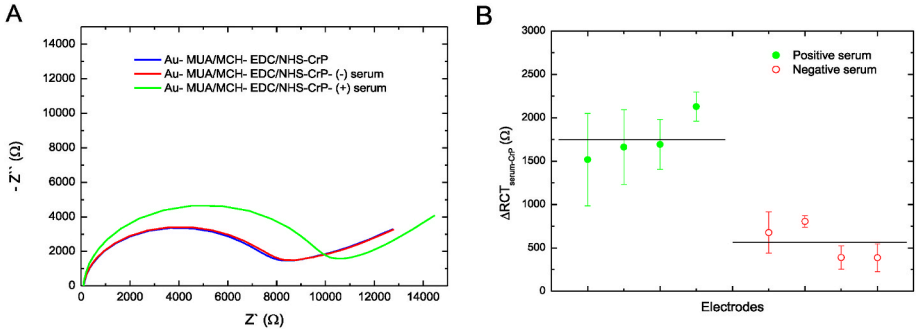

Fig. 4. A) A representative Nyquist plot (-Z″ vs. Z′) for MUA/MCH-EDC/NHS–CrP Au sensor platform before (blue curve) and after incubation with negative (red curve) and positive (green curve) serum. B) $R_{ct,serum} - R_{ct,CrP}$ of the fabricated CrP immunosensor in the presence of (●) infected human serum samples and (○) non-infected human serum samples (error bars represent the SD obtained for three independent experiments on each of the sensors). (For interpretation of the references to colour in this figure legend, the reader is referred to the Web version of this article.)

editing, Supervision, Funding acquisition.

Declaration of competing interest

The authors declare that they have no known competing financial interests or personal relationships that could have appeared to influence the work reported in this paper.

Data availability

Data will be made available on request.

Acknowledgments

The authors acknowledge support from the Royal Society – International Exchanges scheme (IEC\R2\181049), Consejo Nacional de Investigaciones Científicas y Técnicas (CONICET) (PIP 0671 and PUE 22920170100100CO), Universidad Nacional de La Plata (PID 11/X861) and Agencia Nacional de Promoción Científica y Tecnológica-Ministerio de Ciencia, Tecnología e Innovación Productiva (PICT 2016–0679). J.S.C. is member of the investigation support career of CONICET. C.Y.C. and M.A.D.M. are members of the research career of CONICET. M.E.V. is member of the research career of CIC PBA.

References

Balouz, V., Agüero, F., Buscaglia, C.A., 2017. Chapter one - Chagas disease diagnostic applications: present knowledge and future steps. In: Rollinson, D., Stothard, J.R. (Eds.), Advances in Parasitology. Academic Press, pp. 1–45.
Campuzano, S., Pedrero, M., Montemayor, C., Fatás, E., Pingarrón, J.M., 2006. J. Electroanal. Chem. 586 (1), 112–121.
Cazorla, S.I., Frank, F.M., Becker, P.D., Arnaiz, M., Mirkin, G.A., Corral, R.S., Guzmán, C. A., Malchiodi, E.L., 2010. J. Infect. Dis. 202 (1), 136–144.
Cazzulo, J.J., Stoka, V., Turk, V., 1997. Biol. Chem. 378 (1), 1–10.
Cerny, N., Bivona, A.E., Sanchez Alberti, A., Trinitario, S.N., Morales, C., Cardoso Landaburu, A., Cazorla, S.I., Malchiodi, E.L., 2020. Frontiers in Immunology, vol. 11.
Chain, C.Y., Pires Souto, D.E., Sbaraglini, M.L., Labriola, C.A., Daza Millone, M.A., Ramirez, E.A., Cisneros, J.S., Lopez-Albizu, C., Scollo, K., Kubota, L.T., Ruiz, A.M., Vela, M.E., 2019. ACS Infect. Dis. 5 (11), 1813–1819.
Chen, H., Mei, Q., Jia, S., Koh, K., Wang, K., Liu, X., 2014. Analyst 139 (18), 4476–4481.
Cordeiro, T.A.R., Martins, H.R., Franco, D.L., Santos, F.L.N., Celedon, P.A.F., Cantuária, V.L., de Lana, M., Reis, A.B., Ferreira, L.F., 2020. Bios.Bioelectron. 169, 112573.
Diniz, F.B., Ueta, R.R. da C., Pedrosa, A.M., Areias M, da C., Pereira, V.R.A., Silva, E.D., da Silva, J.G., Ferreira, A.G.P., Gomes, Y.M., 2003. Bios.Bioelectron 19 (2), 79–84.
Flores-Chavez Maria, D., Sambri, V., Schottstedt, V., Higuera-Escalante Fernando, A., Roessler, D., Chaves, M., Laengin, T., Martinez, A., Fleischer, B., 2018. J. Clin. Microbiol. 56 (5), e01446, 01417.
Giordanengo, L., Guiñazú, N., Stempin, C., Fretes, R., Cerbán, F., Gea, S., 2002. Eur. J. Immunol. 32 (4), 1003–1011.
Hermanson, G.T., 1997. Bioconjugate Techniques. Academic Press, San Diego, CA.
Hushegyi, A., Bertok, T., Damborsky, P., Katrlik, J., Tkac, J., 2015. Chem.Comm. 51 (35), 7474–7477.
Ibau, C., Arshad, M.K.M., Gopinath, S.C.B., Nuzaihan, M.N.M., Fathil, M.F.M., Shamsuddin, S.A., 2020. Int. J. Biol. Macromol. 162, 1924–1936.
Labriola, C., Sousa, M., Cazzulo, J.J., 1993. Biol. Res. 26 (1–2), 101–107.
Leva-Bueno, J., Peyman, S.A., Millner, P.A., 2020. Med. Microbiol. Immunol. 209 (3), 343–362.
Lidani, K.C.F., Andrade, F.A., Bavia, L., Damasceno, F.S., Beltrame, M.H., Messias-Reason, I.J., Sandri, T.L., 2019. Front. Public Health 7 (166).
Malchiodi, E.L., Chiaramonte, M.G., Taranto, N.J., Zwirner, N.W., Margni, R.A., 1994. Clin. Exp. Immunol. 97 (3), 417–423.
Martinez, J., Campetella, O., Frasch, A.C., Cazzulo, J.J., 1991. Infect. Immun. 59 (11), 4275–4277.
Murta, A.C.M., Persechini, P.M., Padron, T.d.S., de Souza, W., Guimarães, J.A., Scharfstein, J., 1990. Mol. Biochem. Parasitol. 43 (1), 27–38.
Rassi Jr., A., Rassi, A., Marin-Neto, J.A., 2010. Lancet 375 (9723), 1388–1402.
Santos, C.S., Mossanha, R., Wohnrath, K., Inaba, J., Pessôa, C.A., 2016. J. Electrochem. Soc. 163 (5), B158–B162.
Singh, N.K., Arya, S.K., Estrela, P., Goswami, P., 2018. Bios.Bioelectron. 117, 246–252.
Sypabekova, M., Jolly, P., Estrela, P., Kanayeva, D., 2019. Bios.Bioelectron. 123, 141–151.
World Health, O., 2010. Anti-trypanosoma Cruzi Assays: Operational Characteristics, Report 1. World Health Organization, Geneva.